

PHASE VARIATION FOR SNAKE MATCHING IN THE EIC'S HSR

E. Hamwi^{*,1}, G. H. Hoffstaetter^{1,2}, K. Hock², H. Huang²

¹CLASSE, Cornell University, Ithaca, NY, USA

²Collider-Accelerator Department, Brookhaven National Laboratory, Upton, NY, USA

Abstract

The Hadron Storage Ring of the Electron-Ion Collider will feature 6 Siberian snakes placed at the start of each arc to coherently cancel spin precession from diametrically opposite arcs in the ring. To avoid spin-orbital resonances, the alternating sum of the rotation axes of all snakes is 90° , ensuring the closed-orbit spin tune is $\frac{1}{2}$ and sufficiently far away from betatron tunes and integer tunes. This choice does not account for amplitude-dependent spin tune (ADST) shift, which introduces high-order spin orbit resonances in the vicinity of strong first-order resonances. By varying betatron phase advances across each of the 6 arcs, we minimize the strength of first-order spin-orbit resonances as well as ADST shift. In the case of uncooled helium-3, we find it is necessary to minimally vary the vertical orbital tune as well but are able to completely avoid depolarization throughout the ramp with time-dependent phase advances.

INTRODUCTION

The acceleration and preservation of polarization in high-energy hadron beams remains a central challenge in modern accelerator physics. Since first collisions at 255 GeV, the Relativistic Heavy Ion Collider (RHIC) has shown that > 50% proton polarization can be maintained through Siberian snakes and careful lattice symmetry [1, 2]. Building on this legacy, the Hadron Storage Ring (HSR) of the forthcoming Electron-Ion Collider (EIC) will push polarized protons to 275 GeV and, for the first time at comparable energies, accelerate polarized helions (${}^3\text{He}$) to roughly 180 GeV per nucleon [3]. Although the HSR reuses much of RHIC's magnet infrastructure, its two-interaction-point optimization and storage-mode optics break the three-fold symmetry that underpinned RHIC's success.

Six Siberian snakes placed at the start of each arc can enforce a closed-orbit spin tune of $1/2$ when the alternating sum of their rotation axes totals 90° , thereby suppressing first-order imperfection and intrinsic resonances [4]. However, this design does not account for amplitude-dependent spin-tune (ADST) shifts, which seed a dense spectrum of higher-order spin-orbit resonances near strong first-order stopbands. In the absence of electron cooling, especially consequential for helions with large anomalous magnetic moment, these effects threaten depolarization during the energy ramp.

We show that deliberately detuning the betatron phase advances across the six arcs (and for uncooled ${}^3\text{He}$, slightly adjusting the vertical tune) minimizes both first-order coupling and ADST-driven resonance strength. With time-dependent

phase-advance modulation throughout the ramp, we achieve essentially lossless polarization transmission for the studied cases.

SPIN–ORBIT RESONANCES AND SNAKES

Spin Resonances

Closed-orbit spin precession is characterized by the spin tune $v_0 = G\gamma$. *Imperfection resonances* occur when $v_0 \in \mathbb{Z}$ due to closed-orbit errors, while vertical betatron motion drives *intrinsic resonances* when

$$v_0 \pm Q_y \in \mathbb{Z}. \quad (1)$$

In a linearized treatment, the one-turn effect of such resonant precession defines a *spin–orbit coupling* integral. Writing $\vec{\omega} = \vec{\Omega} - \vec{\Omega}_0$ and $\Psi(s) = \int_0^s \vec{\Omega}_0 \cdot \vec{n}_0 \, ds$, the leading contribution reads

$$\begin{aligned} \Delta(s_x + is_y) &\propto \oint [\vec{\omega}(s) \cdot (\hat{x} + i\hat{z})] e^{-i\Psi(s)} \, ds \\ &\approx (G\gamma + 1) \oint k(s) \sqrt{\beta_y(s)} e^{\pm i\phi_y(s)} e^{-i\Psi(s)} \, ds, \end{aligned} \quad (2)$$

where $k = (B\rho)^{-1} dB_y/dx$, and β_y, ϕ_y are the vertical lattice functions.

Snake Magnets

Conceived by Derbenev and Kondratenko [5, 6], Siberian snakes rotate the spin by 180° around a horizontal axis. With pairs of diametrically opposite snakes and vanishing net dipole-driven vertical precession, the closed-orbit spin tune is fixed at

$$v_0 = \frac{1}{2}, \quad (3)$$

independent of energy, thus eliminating first-order resonances.

INVARIANT SPIN FIELD

In stable motion there exists a generalized frame describing off-orbit spin precession, the *invariant frame field* [7]. The corresponding *invariant spin field* (ISF) $\vec{n}(\vec{z}, s)$ obeys

$$\vec{n}(M(\vec{z}), s) = R(\vec{z}, s) \vec{n}(\vec{z}, s), \quad (4)$$

with M the one-turn orbital map and R the one-turn spin rotation. The associated *amplitude-dependent spin tune* (ADST) ν generally differs from the closed-orbit value:

$$\nu \neq v_0 = \frac{1}{2}. \quad (5)$$

* eh652@cornell.edu

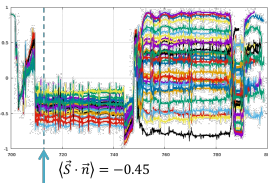


Figure 1: Averaged vertical spin component $\langle S_y \rangle$ for each particle: base lattice (left) vs. with optimized phase trombones (right).

HIGHER-ORDER RESONANCES

Nonlinearities in the coupling integrals generate higher-order spin-orbit resonances, including *snake resonances* that can create discontinuities in the ISF for specific vertical tunes [8]. A generic resonance condition is

$$\nu + j_x Q_x + j_y Q_y + j_z Q_z = k, \quad j, k \in \mathbb{Z}. \quad (6)$$

Higher-order stopbands cluster near strong first-order ones; confirming their impact typically requires non-perturbative methods (e.g., stroboscopic averaging, SODOM-2) [9, 10].

SNAKE MATCHING

Simulations with six diametrically opposite snakes indicate protons can be accelerated to top energy without polarization loss [4], whereas helions face stronger challenges [11]. Following *snake matching* [12, 13], we mitigate higher-order effects indirectly by minimizing the spin-orbit coupling integrals that, in the absence of snakes, quantify first-order resonance strength. Although snakes set $\nu_0 = 1/2$, residual coupling tracks higher-order depolarizing tendencies.

Equation (2) suggests two levers: vary the spin phase $\Psi(s)$ via snake axes [12], or vary $\phi_y(s)$ via quadrupoles. We focus on phase-advance control, which is simpler operationally and avoids extreme snake currents.

INJECTION LATTICE OPTIMIZATION

We study the HSR injection lattice [14, 15] (1-IP, $\beta^* = (\beta_x^*, \beta_y^*) = (5 \text{ m}, 45 \text{ cm})$ at IP6). To scan arc-by-arc phase advances without disturbing β -functions, we introduce idealized *phase trombones* (linear 4×4 blocks at arc quads). An optimization minimizes the coupling integrals at selected energies near strong first-order stopbands. Polarization transport is then evaluated for a 4D bunch at ramp rate $\dot{\gamma} = 0.75/\text{s}$.

Cooled helions show no polarization loss in this configuration, but uncooled beams at 2σ vertical emittance depolarize near $G\gamma \sim 705$. Phase-trombone optimization targeted to this region improves the ISF-projected bunch polarization $\langle \vec{S} \cdot \vec{n} \rangle$ from -0.45 to 0.36 (Fig. 1).

A tune-energy scan of the time-averaged polarization $P_{\lim} \equiv \langle \vec{n}(\vec{z}) \rangle$ identifies narrow safe regions (Fig. 2). Both the base and corrected lattices cross higher-order bands at the nominal $Q_y = 29.210$, but a gap appears near $Q_y \approx 29.125$ for the corrected case, where the ADST distribution tightens toward $\nu \rightarrow 1/2$.

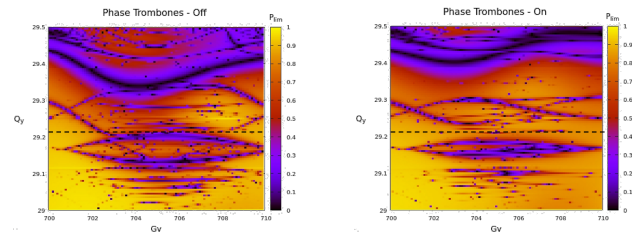


Figure 2: Maximum P_{\lim} ($J_x = 2.5 \pi \mu\text{m}$, $J_y = 5 \pi \mu\text{m}$) across tune-energy space. Dashed line: nominal $Q_y = 29.210$. Left: base; right: with phase trombones. Dark bands indicate higher-order resonances.

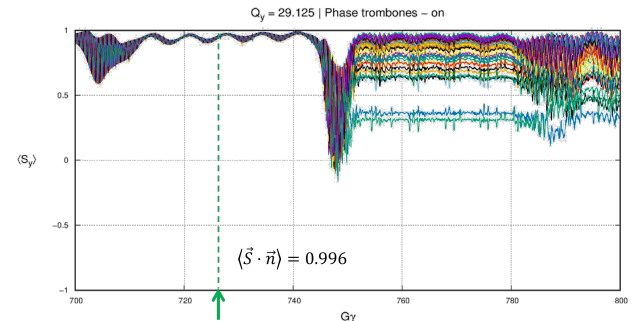


Figure 3: Averaged $\langle S_y \rangle$ for the bunch at the new working point $Q_y = 29.125$ with phase trombones.

Tracking at $Q_y = 29.125$ with phase trombones shows strong recovery of polarization (Fig. 3), and alternating among three phase-trombone settings across $G\gamma \sim 705, 745, 790$ transports 99.4% of polarization from $G\gamma = 700$ to 800 (Fig. 4).

We note that $Q_y = 29.125$ lies on an eighth-order vertical orbital resonance and close to the integer 29, and also satisfies a fourth-order snake-resonance condition. It is therefore prudent not to dwell at this working point outside the targeted energy windows.

CONCLUSION

We analyzed polarization transport for helions across the most dangerous energy interval of the EIC HSR. For cooled beams in the 2-IP store lattice, minor adjustments of the vertical phase advance in two arcs suffice for high transmission,

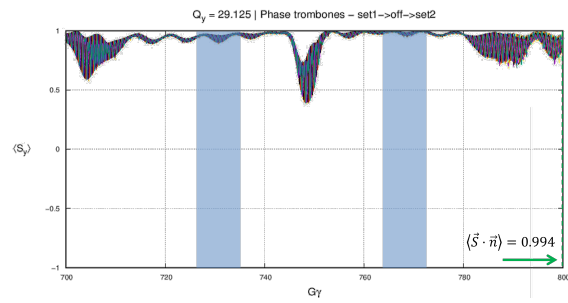


Figure 4: Bunch $\langle S_y \rangle$ with $Q_y = 29.125$ using three phase-trombone settings; shaded intervals indicate linear interpolation between settings.

consistent with prior 1-IP results. For uncooled beams, we turned to the injection lattice and employed arc-wise phase-advance control via idealized trombones, complemented by a modest vertical-tune shift. Alternating time-dependent phase settings across three energy regions yielded 99.4% polarization transmission from $G\gamma = 700$ to 800. While we did not vary snake rotation axes to limit parameter space and to avoid impractical magnet currents, future optimizations that include these variables should further enlarge polarization margins.

ACKNOWLEDGEMENT

I would like to thank Vadim Ptitsyn, Vahid Ranjbar, and Vincent Schoefer for helpful discussions about polarization transmission, and further thanks to J. Scott Berg and Henry Lovelace III for helpful discussions about lattice implementation and providing the accelerator lattices. Finally, I would like to thank David Sagan for his tireless efforts in building and supporting the Bmad simulation library [16], without which this work would not have been possible. This work has been supported by Brookhaven Science Associates, LLC under Contract No. DE-SC0012704 with the U.S. Department of Energy, and No. DE-SC0018008.

REFERENCES

- [1] I. Alekseev *et al.*, “Polarized proton collider at RHIC”, *Nucl. Instrum. Methods Phys. Res., Sect. A*, vol. 499, pp. 392–414, 2003. doi:10.1016/S0168-9002(02)01946-0
- [2] M. Bai *et al.*, “Accelerating polarized protons to 250 GeV”, in *Proc. PAC'07*, Albuquerque, NM, USA, Aug. 2007, pp. 745–747. doi:10.1109/PAC.2007.4440761
- [3] J. Berg *et al.*, “Lattice design for the hadron storage ring of the Electron-Ion Collider”, in *Proc. IPAC'23*, Venice, Italy, May 2023, pp. 903–905. doi:10.18429/JACoW-IPAC2023-MOPL156
- [4] H. Huang *et al.*, “Strategy for proton polarization in the Electron Ion Collider”, in *Proc. IPAC'23*, Venice, Italy, May 2023, pp. 523–526. doi:10.18429/JACoW-IPAC2023-MOPL011
- [5] Y. S. Derbenev and A. M. Kondratenko, “Acceleration of polarized particles to high energies in synchrotrons”, in *Proc. 10th International Conference on High Energy Accelerators*, Protvino, USSR, Jul. 1977, pp. 70–75. <https://cds.cern.ch/record/472401>
- [6] Y. S. Derbenev and A. M. Kondratenko, “On the possibilities to obtain high-energy polarized particles in accelerators and storage rings”, *AIP Conf. Proc.*, vol. 51, pp. 292–306, 1979. doi:10.1063/1.31775
- [7] D. P. Barber, J. A. Ellison, and K. Heinemann, “Quasiperiodic spin-orbit motion and spin tunes in storage rings”, *Phys. Rev. Spec. Top. Accel Beams*, vol. 7, no. 12, p. 124 002, 2004. doi:10.1103/PhysRevSTAB.7.124002
- [8] E. Hamwi and G. H. Hoffstaetter, “Higher-order spin depolarization analysis”, in *Proc. IPAC'23*, Venice, Italy, May 2023, pp. 3133–3135. doi:10.18429/JACoW-IPAC2023-WEPL014
- [9] G. H. Hoffstaetter, M. Vogt, and D. P. Barber, “Higher-order effects in polarized proton dynamics”, *Phys. Rev. Spec. Top. Accel Beams*, vol. 2, no. 11, p. 114 001, 1999. doi:10.1103/PhysRevSTAB.2.114001
- [10] K. Yokoya, “An Algorithm for calculating the spin tune in circular accelerators”, Feb. 1999, arXiv:physics/9902068 [physics.acc-ph]. doi:10.48550/arXiv.physics/9902068
- [11] K. Hock, E. Hamwi, F. Meot, H. Huang, and V. Ptitsyn, “Simulations of polarized helions in the HSR”, in *Proc. IPAC'24*, Nashville, TN, USA, May 2024, pp. 1634–1636. doi:10.18429/JACoW-IPAC2024-TUPS05
- [12] G. H. Hoffstaetter, “Optimal axes of siberian snakes for polarized proton acceleration”, *Phys. Rev. Spec. Top. Accel Beams*, vol. 7, no. 12, p. 121 001, 2004. doi:10.1103/PhysRevSTAB.7.121001
- [13] E. Hamwi, G. Hoffstaetter, H. Huang, K. Hock, and V. Ptitsyn, “Snake matching the EIC's hadron storage ring”, in *Proc. IPAC'24*, Nashville, TN, USA, May 2024, pp. 1714–1717. doi:10.18429/JACoW-IPAC2024-TUPS33
- [14] H. L. III *et al.*, “Hadron Storage Ring 4 O'clock Injection Design and Optics for the Electron-Ion Collider”, in *Proc. IPAC'22*, Bangkok, Thailand, Jun. 2022, pp. 2068–2070. doi:10.18429/JACoW-IPAC2022-WEPOTK014
- [15] H. L. III *et al.*, “The Electron-Ion Collider Hadron Storage Ring 10 O'clock Switchyard Design”, in *Proc. IPAC'22*, Bangkok, Thailand, Jun. 2022, pp. 2071–2073. doi:10.18429/JACoW-IPAC2022-WEPOTK015
- [16] D. Sagan, “Bmad: A relativistic charged particle simulation library”, *Nucl. Instrum. Methods Phys. Res., Sect. A*, vol. A558, no. 1, pp. 356–359, 2006. doi:10.1016/j.nima.2005.11.001